Counterion Effects on Ion Mobility and Mobile Ion Concentration of Doped Polyphosphazene and Polyphosphazene Ionomers

Robert J. Klein,[†,‡] Daniel T. Welna,[§,||] Arlin L. Weikel,[§] Harry R. Allcock,[§] and James Runt*[,†]

Department of Materials Science and Engineering and the Materials Research Institute and Department of Chemistry, The Pennsylvania State University, University Park, Pennsylvania 16802

Received February 11, 2007; Revised Manuscript Received March 20, 2007

ABSTRACT: A physical model of electrode polarization is applied to dielectric (impedance) data from two poly(methoxyethoxy−ethoxy phenoxyphosphazene) systems with nearly identical chemical structures, one composed of an ionomer with a single mobile cation and the other composed of a salt-doped polymer with mobile cation and mobile anion. Quantitative comparison of the ion mobility and mobile ion concentration, based on chemical structure, is achieved. Both conductivity and ion mobility are reduced to common curves by normalizing T with T_g, indicating that T_g of the polymer matrix is a major factor controlling ion diffusion. Even with the use of normalized temperature, both the mobility of ions and the mobile ion concentration in the doped polymers are ∼10 times larger than those in the ionomers. These factors arise from faster diffusion of the anion and the local environment surrounding ion pairs. Also, Arrhenius and VFT parameters associated with mobile ion concentration and ion mobility, respectively, reveal differences in activation energies between ionomer and doped polymer that are due to interactions between the ion pairs and polymer segments.

1. Introduction

Improvement of high-density chemical sources of energy remains the most significant challenge for mobile technology. Energy storage devices such as batteries and fuel cells deliver energy by transport of ions through a polymer membrane. Improvements in polymer membranes for ion transport have been achieved in recent years by the engineering of improved gel polymer electrolytes,[1] but the fundamental mechanisms that govern ion transport through polymers are still not well-understood after 30 years of research.[2,3]

Recent simulations of "simple" ion-containing systems and experiments on carefully designed polymers have improved understanding of the transport mechanisms. Borodin and Smith recently presented a detailed molecular dynamics simulation that predicts three separate lithium transport pathways for lithium salts in poly(ethylene oxide) (PEO).[4] The effects of counterion size on conductivity, especially in light of the relative mobilities of the cation and anion, have been investigated by Kato et al. for a PEO-based ionomer.[5] Sadoway and co-workers demonstrated the intriguing result that chemically distancing ion-containing groups from PEO-based regions actually enhanced the overall conductivity.[6,7] The strong effect of T_g on conductivity in plasticized systems with no phase separation was demonstrated by Zhang et al.[8]

Despite these advances, the underlying components of conductivity—ion mobility and mobile ion concentration—must be decomposed and understood *individually* before theoretical development can continue. This paper addresses these two components of conductivity by utilizing a physical model of electrode polarization,[9,10] recently refined and demonstrated to be valid for ionomers,[11] and applying this model to data from dielectric (impedance) spectroscopy. Equally important to this study, ionomers (containing a single type of mobile ion) and polymers doped with salt (containing both mobile cations and anions) of virtually identical chemical makeup are compared and contrasted. Because of the nearly identical chemical structure, quantitative analysis of the conduction parameters pinpoints the mechanisms and primary factors influencing ion transport.

This present work, which utilizes poly(methoxyethoxy−ethoxy phenoxyphosphazene), also complements previous studies of poly(methoxyethoxy−ethoxy phosphazene) doped with lithium salts, where it was found that the vast majority of ions exist in a bound state.[12] It has also been proposed that lithium cations are most stable when coordinated simultaneously by one backbone nitrogen and several pendant ether oxygens.[13] In addition, the present work serves as a valuable continuation of the study of conductivity parameters of ionomers. Previously,[11] measurement of ion mobility and mobile ion concentration for a simple PEO-based ionomer demonstrated, among other results, that mobile ion concentration is a tiny fraction of the total ion concentration. Similar results will be shown for the poly(methoxyethoxy−ethoxy phenoxyphosphazene)-based ionomers, and through the use of both a salt-doped polymer with nearly identical chemical makeup and variations in ion stoichiometry, it is possible to quantify the fraction of mobile ions in terms of the chemical structure available for coordination.

2. Experimental Method

Two types of conductive poly(methoxyethoxy−ethoxy phenoxyphosphazene) are under consideration. One is a doped polymer where lithium bis(trifluoromethanesulfonyl)imide (LiTFSI) is used as a dopant (system D). The other is an ionomer, where a small molecule very similar to LiTFSI is covalently bonded to the phosphazene backbone (system I). The amount of salt and the number of anionic groups bound to the main chain were selectively controlled, thereby establishing two pairs of systems with nearly identical chemical compositions. Figure 1 provides the chemical structure, and Table 1 lists the pertinent properties.

[†] Department of Materials Science and Engineering and the Materials Research Institute, The Pennsylvania State University.

[‡] Present address: Organic Materials Department, Sandia National Laboratories, Albuquerque, NM.

[§] Department of Chemistry, The Pennsylvania State University.

[||] Present address: Air Force Research Laboratory (AFRL/MLBP), Wright-Patterson Air Force Base, OH.

10.1021/ma070357o CCC: $37.00
Published on Web 04/19/2007

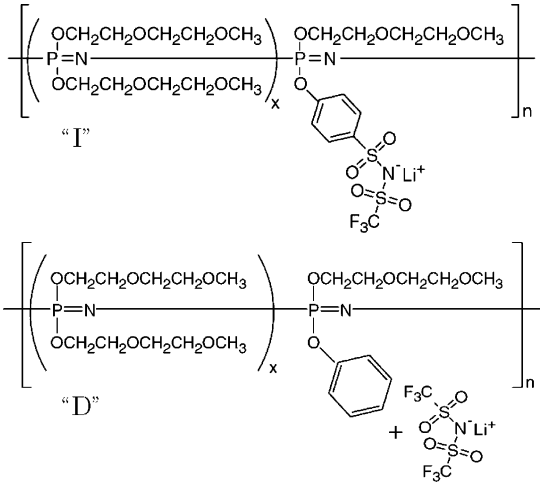

Figure 1. Chemical structures of poly(methoxyethoxy−ethoxy phenoxyphosphazene)-based ionomer (I) and doped poly(methoxyethoxy−ethoxy phenoxyphosphazene) (D).

Table 1. Important Ionomer (I-17 and I-9) and Doped Polymer (D-15 and D-10) Properties, Including the Ratio of Ions to Ether Oxygen Segments, Glass Transition Temperature, Number Average Molecular Weight, Polydispersity Index, and Stoichiometric Concentration of Total Lithium Ions[14]

sample	ions/(EO)$_3$ mol %	T_g (°C)	M_n (kg/mol)	PDI	[Li$^+$] ions/cm^3
I-17	17	−32	150	2.8	5.4×10^{20}
I-9	9	−45	150	2.8	3.0×10^{20}
D-15	15	−69	130	2.7	4.8×10^{20}
D-10	10	−73	130	2.7	3.4×10^{20}

Both polymers were synthesized by methods described in a previous publication by Allcock et al.[14] Species I was prepared by the following route. The small molecule 4-hydroxy-*N*-[(trifluoromethyl)sulfonyl]-benzenesulfonamide disodium salt was covalently attached, via nucleophilic substitution, to the phosphazene backbone. The sodium ions were then exchanged for lithium ions to produce the ionomers. The resulting polymers were purified and NMR was used to confirm the molecular structure. Throughout this paper, I-17 and I-9 refer to ionomers with 17 mol % and 9 mol % of the methoxyethoxy−ethoxy segments substituted for ion-containing groups, respectively. D-15 and D-10 indicate the doped polymer where 15 and 10 mol % pendant phenoxy groups replace methoxyethoxy−ethoxy segments, respectively, and 15 and 10 mol % LiTFSI were added. Gel permeation chromatography established the molecular weights and polydispersity indices. The glass transition temperatures T_g were obtained from differential scanning calorimetry. For both the ionomers and the doped polymers, the addition of ions dramatically influences T_g, which increases from −84 °C for neat poly(methoxyethoxy−ethoxy phenoxyphosphazene) to the values seen in Table 1. Increases in T_g with ion content commonly appear in polymer−salt mixtures,[15] and they are even more pronounced in ionomers.[16,17] Further details on measurements of the polymer characteristics are provided in Allcock et al.[14] The chemical composition of the doped polymers is $[NP((OCH_2CH_2)_2OCH_3)_x(OC_6H_5)_y]_n + yLi^+[(CFSO_2)_2N]^-$, and the ionomers contain $[NP((OCH_2CH_2)_2OCH_3)_x(OC_6H_4SO_2N(Li)SO_2CF_3)_y]_n$, as represented in Figure 1.

Dielectric (impedance) spectra were collected isothermally using a Novocontrol GmbH Concept 40 broadband dielectric spectrometer in the frequency range 10^{-2}−10^6 Hz. Temperatures were controlled to within 0.2 °C and the time-averaged temperature during each frequency sweep was recorded. Electrodes consisted of polished brass circular plates coated with gold. Samples for dielectric spectroscopy were prepared by carefully drying the polymers and spacers on the electrodes in a vacuum oven at 70 °C for at least 8 h and squeezing the electrodes to the desired thickness.

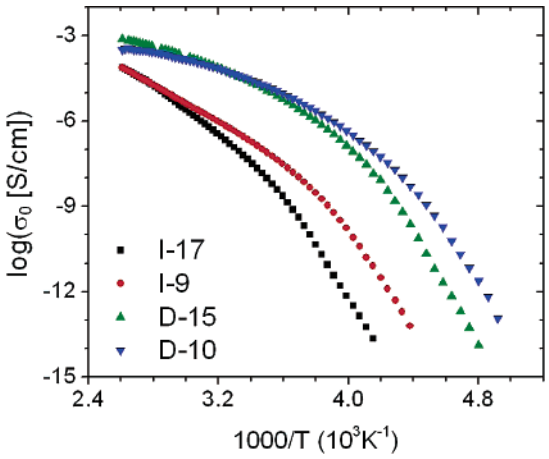

Figure 2. Temperature dependence of conductivity for the ion-containing polymers under consideration. Error bars are smaller than the size of the data points.

Small-angle X-ray scattering (SAXS) patterns were collected using a Molecular Metrology instrument equipped with a Cu target ($\lambda = 1.542$ Å) and a two-dimensional area, proportional counter. Scattering data were collected for 6 h.

3. Results and Discussion

3.1. Results and Analysis. Dc conductivities were evaluated from the linear portion (in a log−log plot) of the dielectric loss ϵ'' as a function of frequency f by

$$\epsilon'' = \left(\frac{\sigma_0}{\epsilon_{vac}\omega}\right)^n \quad (1)$$

where ϵ_{vac} is the vacuum permittivity, $\omega = 2\pi f$ is the radial frequency, and $0.9 < n \leq 1.0$ is the conductivity exponent. As n approaches 1, the ideal ion drift is active, whereas lower values indicate tortuous conduction paths.[18] In the systems under investigation, n is very close to 1 at higher temperatures, but close to T_g, the polymer dynamics slow down, constricting conduction paths and leading to a decrease in n. In the data sets under consideration, $n > 0.9$ for $T > T_g + 15$ K and $n > 0.98$ for $T > T_g + 25$ K. σ_0 was obtained by fitting eq 1 to the six data points that maximized n for a particular temperature. This region that maximizes n is chosen to avoid the effects of electrode polarization at low frequency and the ac-to-dc conductivity transition at high frequency.

Values of dc conductivity σ_0 as a function of temperature for I-17, I-9, D-15, and D-10 are plotted in Figure 2. For these ion concentrations, higher ion content leads to lower conductivity at all but the highest temperatures.

As noted above, adding more ions increases T_g, due to polymer-ion interactions.[15−17,19] The first step toward understanding the polymer mechanisms that promote conduction is to remove the effect of T_g. Many previous investigations[e.g.,8,20,21] have found T_g to be a central factor controlling conductivity. As Figure 3 indicates, T_g is a very important factor here as well: changing the independent variable to the normalized temperature $T - \Delta T_g$ collapses the ionomer and doped polymer data sets onto two master curves. ΔT_g is the relative difference in T_gs, defined here as $T_g - T_0$, with $T_0 = 273.15$ K arbitrarily chosen to avoid distortion in the Arrhenius plots. Far above T_g, the presence of more ions becomes a slightly stronger influence than the concurrent increase in T_g, and the conductivities of I-17 and D-15 respectively surpass those of I-9 and D-10.

To understand the differences between the conductivities of the ionomers and doped polymers, it is necessary to understand

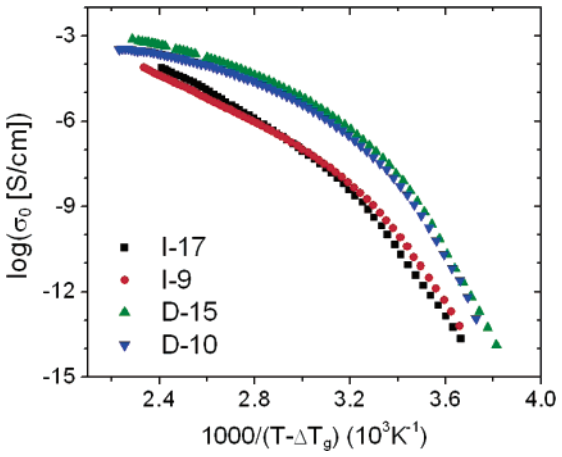

Figure 3. Conductivities as a function of $T - \Delta T_g$ for the ionomers and doped polymers under consideration. Error bars are smaller than the size of the data points.

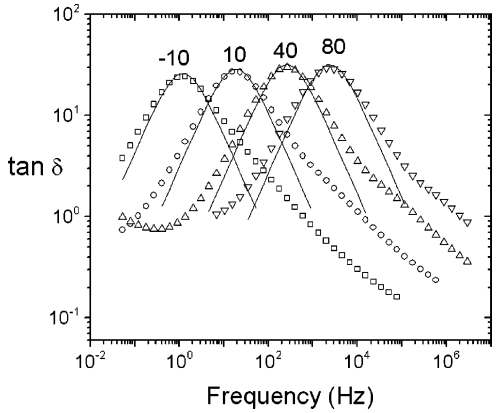

Figure 4. Macroscopic relaxations arising from electrode polarization for I-9 are evident in tan δ (f) for temperatures from −10 to +80 °C. tan δ for I-17 has a very similar appearance. The solid lines represent fits by eq 4. Error bars are smaller than the size of the data points.

the root components of conductivity. Ionic conductivity at its fundamental level is a function of the speed and number of active species, and therefore is written

$$\sigma_0 = \sum_{\text{positive carriers } i} p_i q \mu_i + \sum_{\text{negative carriers } j} n_j q \mu_j \qquad (2)$$

where p is the positive carrier concentration, n is the negative carrier concentration, and μ is the carrier mobility for any particular charged species. Working under the assumption that there are only two charged species that contribute significantly to the conductivity, eq 2 simplifies to

$$\sigma = p_0 q \mu_+ + n_0 q \mu_- \qquad (3)$$

In the doped polymers, the assumption that triple ions—e.g., $(Li_2TFSI)^+$—do not contribute to conductivity is rationalized based on two facts. First, the stoichiometric ion concentration is ~1% that of $P(EO)_4$:$LiClO_4$, in which triple ions have been shown to be responsible for a minor portion of the conductivity.[22] Lower concentrations significantly reduce ion−ion interactions and ionic aggregates.[12] Second, the bulky anion $TFSI^-$, where the negative charge is delocalized across the molecule, encourages the dissociation of ionic pairs to some degree.[23,24] In the ionomer, of course, the negative anionic species are bound to the polymer, restricting their motion sufficiently so that $\mu_- \ll \mu_+$.[6]

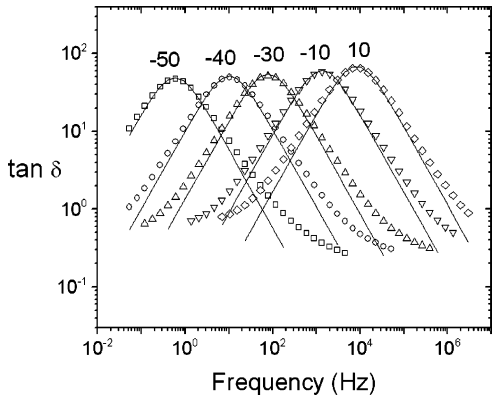

Figure 5. Macroscopic relaxations arising from electrode polarization for D-10 are evident in tan δ (f) for temperatures from −50 to +10 °C. tan δ for D-15 has a very similar appearance. The solid lines represent fits by eq 4. Error bars are smaller than the size of the data points.

As long as a single ionic species dominates conductivity, and ion concentrations are relatively low so that diffusing ions do not strongly interfere with each other, the electrode polarization that is created upon applying low-frequency fields across blocking electrodes can be modeled as a simple macroscopic Debye relaxation, as described in a previous publication.[11] Data in tan $\delta = \epsilon''/\epsilon'$ as a function of frequency can then be modeled by

$$\tan \delta = \frac{2\pi f \tau_{EP}}{1 + (2\pi f \tau_{EP})^2/M} \qquad (4)$$

where f is frequency and τ_{EP} and M are fitting parameters. Ion mobility μ is then obtained directly as

$$\mu = \frac{qL^2}{4M \tau_{EP} kT} \qquad (5)$$

and mobile ion concentration p_0 from

$$p_0 = \frac{\sigma_0}{q\mu} \qquad (6)$$

The fitting of eq 4 to peaks in tan δ of I-9 is shown in Figure 4.

Electrode polarization of the polymer + salt system would appear to be more complicated, since at least two ionic species—Li^+ and $TFSI^-$—can contribute simultaneously to the conductivity. However, tan δ (f) of both D-10 (Figure 5) and D-15 reveal no broadening or doublets. There are three possible scenarios that would result in the behavior seen in Figure 5: $\mu_- = \mu_+$, $\mu_- \ll \mu_+$, or $\mu_- \gg \mu_+$. On the basis of evidence reported in previous investigations[4,5,21,25] that identifies $TFSI^-$ as diffusing much faster than the Li^+ cation, the behavior seen in Figure 5 must arise from $\mu_- \gg \mu_+$. Thus, μ calculated from fits of tan δ is associated with anion motion. Values for free ion concentration via eq 6 are derived from the dominant anion motion, but since every anion is obtained by separation of an ion pair, $n_0 = p_0$.

Ion mobility, derived directly from fitting tan δ, is shown for the four ion conductors in Figure 6. Each data set is fit by the Vogel−Fulcher−Tammann (VFT) relationship[26]

$$\mu = \mu_\infty \exp\left(\frac{-B}{T - T_0}\right) \qquad (7)$$

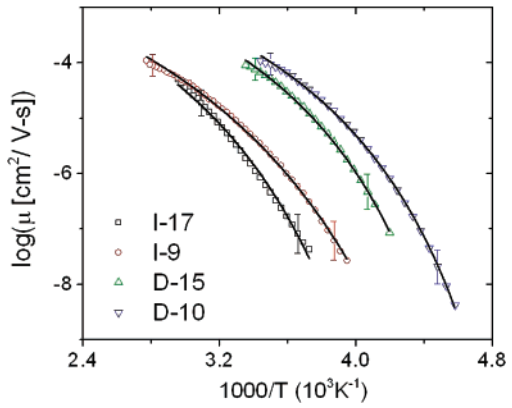

Figure 6. Temperature dependence of ion mobility, obtained from eq 5, with VFT fits by eq 7. Error bars, estimated from duplicate measurements, are ~50%.

Table 2. VFT Parameters for $\mu(T)$ and Arrhenius Activation Energies for $p_0(T)$.

sample	B (K)	T_0 (K)	E_a^{ion} (kJ/mol)
I-17	990 ± 100	195 ± 10	19.8 ± 0.4
I-9	1000 ± 80	186 ± 5	17.7 ± 0.5
D-15	640 ± 50	189 ± 5	14.1 ± 0.8
D-10	670 ± 50	177 ± 5	12.9 ± 0.8

[a] Errors were established by a combination of error of fitting and differences between duplicate measurements.

where T_0 is the Vogel temperature (at which ion mobility goes to zero), B is a constant with units of temperature, and μ_∞ is the infinite-temperature ion mobility. The VFT parameters obtained from fitting $\mu(T)$ are shown in Table 2, with the exception of μ_∞, which was fixed at $10^{-1.3}$ cm^2/(V s), a common method to increase reliability of the three-parameter model.[27]

The parameters listed in Table 2 reveal a surprising relationship: the parameters B for the ionomers are ca. 1.5 times that for the doped polymers. B is representative of the pseudo-activation energy in the Arrhenius (high-temperature) limit of the VFT relation, and in the context of the Doolittle−Cohen free volume theory[26]

$$B = \frac{f^*}{\alpha_f} \tag{8}$$

where f^* is the relative averaged free volume required for transport of a molecule and α_f is the thermal expansion coefficient of the free volume. Since the chemical compositions of ionomers and doped polymers are nearly identical, $\alpha_f^I \approx \alpha_f^D$, and therefore the free volume required for ionic transport is significantly larger for the ionomers than for the doped polymers.

On the other hand, values of T_0 in Table 2 do not have sufficient statistical significance to differentiate between samples. However, T_g, which is related to T_0 and has been measured more precisely, is very significant to ion mobility. In an improvement over reducing conductivity with normalized temperature, plotting $\mu(T - \Delta T_g)$ reduces the data to two common curves, indicating the strong influence of T_g (Figure 7).

$p_0(T)$ is then obtained by way of eq 6 (Figure 8). An Arrhenius relation has previously been established as appropriate for fitting mobile ion concentration:[11,28]

$$p_0 = p_\infty \exp\left(\frac{-E_a}{RT}\right) \tag{9}$$

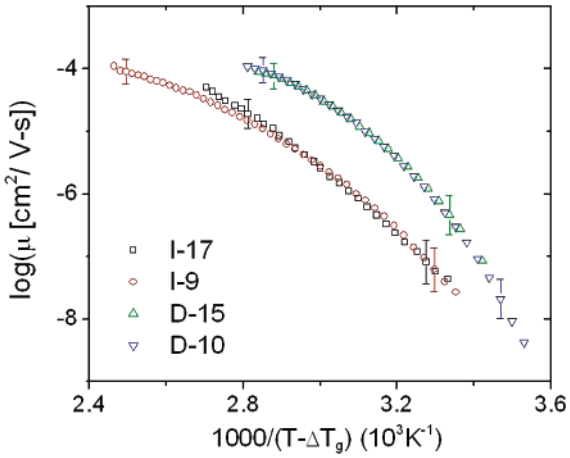

Figure 7. Mobility as a function of $T - \Delta T_g$. Error bars, estimated from duplicate measurements, are ~50%.

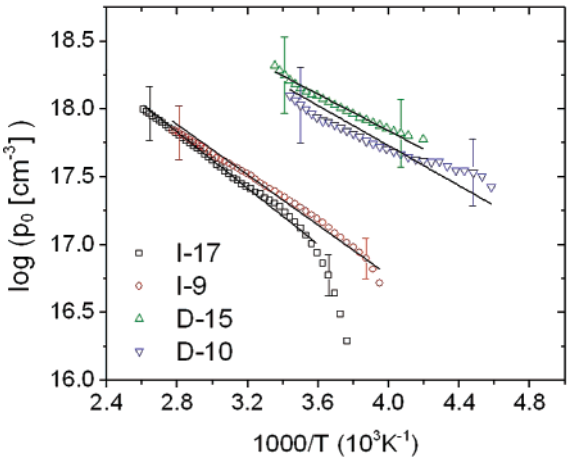

Figure 8. Mobile cation concentration as a function of temperature. Error bars, estimated from duplicate measurements, are ~60%.

where p_∞ is the cation concentration as $T \rightarrow \infty$. At infinite temperature, virtually all of the ion pairs will be separated, so p_∞ can be regarded as equivalent to the stoichiometric ion concentration, and therefore fitting by eq 9 used the values of p_∞ in Table 1. The resulting fits are shown in Figure 8. The fractions of ions involved in conduction p_0/p_∞ are very small, approximately 5×10^{-4} for the ionomers and 3×10^{-3} for the doped polymers at 20 °C. These very small values are in line with observations for a PEO-based ionomer[11] as well as the result that most of the ions in poly(methoxyethyoxy−ethoxy phosphazene)−salt mixtures exist in a bound state.[12]

Finally, the structures of the ionomeric and doped samples were evaluated by SAXS. The results, shown in Figure 9, indicate the presence of a small "ionomer peak" in the ionomers (well-defined for I-17, but also evident as a slight shoulder in I-9), representing clustering of at least some of the ions in the system. Of course, clusters in the ionomers are not directly involved in conduction because anions involved in clusters are covalently attached to the polymer main chains and therefore relatively immobile. There is no such clustering in the doped polymers. SAXS often detects clustering in ionomers with hydrophobic matrices, but previous investigation of a PEO-based ionomer, which has approximately the same ion concentration as the ionomers under consideration here, did not reveal any ionomer scattering peak.[17] The average center-to-center cluster spacing, calculated from $d = 2\pi/q_{max}$, is 39 nm for I-17, relatively large compared to most ionomers.[29] Also, the upturn in scattering intensity at low q is significant. Similar behavior

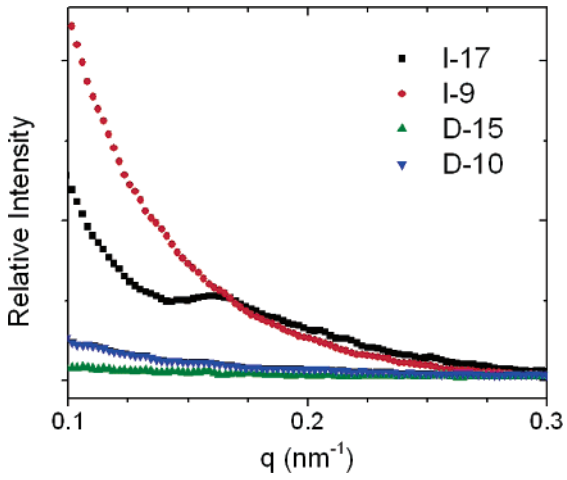

Figure 9. Relative SAXS intensity as a function of scattering vector q for the four ion-containing polymers under consideration, collected at 25 °C.

has been observed previously for ionomers, and it has been proposed that this is associated with long-range inhomogeneity of the spatial distribution of the metal ions.[30,31]

3.2. Discussion. The importance of T_g on ion motion has been demonstrated in the plots of μ and σ_0 as a function of $T - \Delta T_g$ (Figures 3 and 7). There are five additional findings that must be considered, and reconciled, in a broader context: (a) $\mu^D/\mu^I \approx 10$; (b) $f_I^*/f_P^* \approx 1.5$; (c) $p_0^D/p_0^I \approx 10$; (d) $E_a^I/E_a^D \approx 1.4$; and (e) ionic clustering is apparent in the ionomers but not in the doped polymers. Since the chemical structures of the ionomers and the doped polymers are nearly identical, the differences in $\mu(T)$ and $p_0(T)$ must arise from the *location* and *mobility* of the anion.

As documented by Kato et al.,[5] the cationic transference number[22]

$$t_+ = \frac{\mu_+}{\mu_+ + \mu_-} \tag{10}$$

of LiTFSI in PEO-based systems is 0.11, or $\mu_-/\mu_+ = 8$; i.e., the anion moves 8 times faster than the cation. This is supported by other experiments where the anion diffused significantly faster than the cation in a PEO-based polymer electrolyte.[21,25] This explains the larger values of ion mobility in the doped polymer than the ionomer, as well as clarifying that the Debye-shaped peak in Figure 5 arises exclusively from $TFSI^-$. The increase in f^* for the ionomer also most likely arises from Li^+ in the coordinated state requiring more free volume than $TFSI^-$ to diffuse, since Li^+ is surrounded by four to five coordinating ether oxygens.[24]

Also, Sadoway and co-workers[6,7] synthesized a series of Li^+-containing, block copolymer ionomers, where the counteranion was located either in the conductive PEO-based block or in a nonconductive block. Conductivities in the former polymers were 10 to 100 times lower than in the latter, for equivalent stoichiometries. These studies strongly suggest that ions originating near PEO-based regions are held relatively immobile by virtue of interactions between anion, cation, and ether oxygens. In the polymeric system, the unbound $TFSI^-$ anions are free to separate from PEO-rich regions, but in the ionomeric system anions are covalently restricted, and therefore cations are electrostatically restricted, to PEO-rich regions. The significant increase in E_a for the ionomers indicates that such a restriction is energetically less favorable to the formation of free ions than chemically unrestricted ion pairs.

Furthermore, the lower values of ion mobility and higher values of E_a present in the ionomers can be partially attributed to the effect of ion clustering. In ionomers possessing ionic clusters, the coronal chains that surround clusters are dynamically inhibited.[32,33] Clusters of multiple cations-anions will therefore decrease the local chain mobility and thus the ion mobility, and the electrostatic effect of adjacent ions will increase the activation energy for ion pair separation.

4. Summary

By the application of a physical model of electrode polarization to two systems with nearly identical chemical compositions, one composed of an ionomer with a single mobile cation, and the other composed of a salt-doped polymer with mobile cation and mobile anion, quantitative comparison of the conductivity parameters was achieved. Both conductivity $\sigma_0(T)$ and ion mobility $\mu(T)$ are reduced to common curves by normalizing T with T_g, indicating that T_g of the polymer matrix is the primary variable controlling ion diffusion. However, even with the use of normalized temperature, the mobility of ions in the doped system is ~10 times larger than that in the ionomeric system. As indicated by previous investigations of polymer electrolytes, this factor most likely arises from the faster diffusion of the anion $TFSI^-$ than the cation Li^+.

Furthermore, the VFT parameters associated with ion mobility reveal that the free volume required for Li^+ diffusion is 1.5 times that required for $TFSI^-$ diffusion. On the basis of the molecular interactions found in previous investigations of ether oxygen-containing polymer−salt complexes, this noticeable difference in free volume required for diffusion evolves from the coordination of 4 to 5 ether oxygens to each lithium cation. The bulky anion does not bond strongly to the polymer and suffers none of the restrictive bonds of the lithium cation.

Values of mobile ion concentration p_0 also reveal significant differences between the doped polymer and the ionomer. The ionomer has about 10 times fewer mobile ions available for diffusion, and the activation energy is ~1.4 times higher. Since the analytical method separates p_0 from μ, these differences must arise from the local environment surrounding the ion pair. This is supported by the presence of an "ionomer scattering peak" for the two ionomer samples, indicating at least partial ionic clustering, whereas no scattering peak is visible in the doped polymers. The location of the ion pairs in the polymer matrix has a crucial effect on both μ, which can be dynamically restricted by the presence of ionic clusters, and p_0, which is sensitive to the local coordination environment.

These results quantitatively establish that, relative to the doped ionomer, ionomers suffer significant reductions in conductivity, mobility, and mobile ion concentration due to the impact of the fixed cation. In order for ionomers to be utilized as ion transport membranes in functional devices, dramatic changes must be made to the chemistry to either decrease the T_g, create an alternate route for ionic transport, or modify the electrostatic interactions between the covalently bound counterion and the mobile ion.

Acknowledgment. This work was supported by the National Science Foundation, Polymers Program under Grant DMR-0605627. We would like to thank Pornpen Atorngitjawat for helpful discussions on measurement and analysis of the small-angle X-ray scattering and dielectric data.

Supporting Information Available: Figures showing plots of $\epsilon'(f)$ and $\epsilon''(f)$ for I-17, I-9, D-10, and D-15. This material is available free of charge via the Internet at http://pubs.acs.org.

References and Notes

(1) Xu, K. *Chem. Rev.* **2004**, *104*, 4303.
(2) Meyer, W. H. *Adv. Mater.* **1998**, *10*, 439.
(3) Wright, P. V. *MRS Bull.* **2002**, *27*, 597.
(4) Borodin, O.; Smith, G. D. *Macromolecules* **2006**, *39*, 1620.
(5) Kato, Y.; Yokoyama, S.; Yabe, T.; Ikuta, H.; Uchimoto, Y.; Wakihara, M. *Electrochim. Acta* **2004**, *50*, 281.
(6) Sadoway, D. R.; Huang, B. Y.; Trapa, P. E.; Soo, P. P.; Bannerjee, P.; Mayes, A. M. *J. Power Sources* **2001**, *97-8*, 621.
(7) Ryu, S. W.; Trapa, P. E.; Olugebefola, S. C.; Gonzalez-Leon, J. A.; Sadoway, D. R.; Mayes, A. M. *J. Electrochem. Soc.* **2005**, *152*, A158.
(8) Zhang, S. H.; Dou, S. C.; Colby, R. H.; Runt, J. *J. Non-Cryst. Solids* **2005**, *351*, 2825.
(9) MacDonald, J. R. *Phys. Rev.* **1953**, *92*, 4.
(10) Coelho, R. *J. Non-Cryst. Solids* **1991**, *131*, 1136.
(11) Klein, R. J.; Zhang, S. H.; Dou, S.; Jones, B. H.; Colby, R. H.; Runt, J. *J. Chem. Phys.* **2006**, *124*, 144903.
(12) Frech, R.; York, S.; Allcock, H.; Kellam, C. *Macromolecules* **2004**, *37*, 8699.
(13) Luther, T. A.; Stewart, F. F.; Budzien, J. L.; LaViolette, R. A.; Bauer, W. F.; Harrup, M. K.; Allen, C. W.; Elayan, A. *J. Phys. Chem. B* **2003**, *107*, 3168.
(14) Allcock, H. R.; Welna, D. T.; Maher, A. E. *Solid State Ionics* **2006**, *177*, 741.
(15) Lemaitre-Auger, F.; Prud'homme, J. *Electrochim. Acta* **2001**, *46*, 1359.
(16) Gray, F. *Solid Polymer Electrolytes*; VCH Publishers: New York, 1991; pp 95−123.
(17) Dou, S.; Zhang, S. H.; Klein, R. J.; Runt, J.; Colby, R. H. *Chem. Mater.* **2006**, *18*, 4288.
(18) Mauritz, K. A. *Macromolecules* **1989**, *22*, 4483.
(19) Kim, J. H.; Min, B. R.; Won, J.; Kang, Y. S. *J. Phys. Chem. B* **2003**, *107*, 5901.
(20) Besner, S.; Vallee, A.; Bouchard, G.; Prudhomme, J. *Macromolecules* **1992**, *25*, 6480.
(21) Yoshizawa, M.; Ito-Akita, K.; Ohno, H. *Electrochim. Acta* **2000**, *45*, 1617.
(22) Gray, F. *Solid Polymer Electrolytes*; VCH Publishers: New York, 1991; pp 183−214.
(23) Abbrent, S.; Lindgren, J.; Tegenfeldt, J.; Wendsjo, A. *Electrochim. Acta* **1998**, *43*, 1185.
(24) Mao, G. M.; Saboungi, M. L.; Price, D. L.; Armand, M. B.; Howells, W. S. *Phys. Rev. Lett.* **2000**, *84*, 5536.
(25) Bando, T.; Aihara, Y.; Hayamizu, K.; Akiba, E. *J. Electrochem. Soc.* **2004**, *151*, A898.
(26) Kremer, F.; Schonhals, A. In *Broadband Dielectric Spectroscopy*; Kremer, F., Schonhals, A., Eds.; Springer-Verlag: New York, **2003**; pp 99−130.
(27) Atorngitjawat, P.; Klein, R. J.; Runt, J. *Macromolecules* **2006**, *39*, 1815.
(28) Ratner, M. A. In *Polymer Electrolyte Reviews I*; MacCallum, J. R., Vincent, C. A., Eds.; Elsevier Applied Science: New York, 1987; pp 173−236.
(29) Yarusso, D. J.; Cooper, S. L. *Macromolecules* **1983**, *16*, 1871.
(30) Li, Y. J.; Peiffer, D. G.; Chu, B. *Macromolecules* **1993**, *26*, 4006.
(31) Wu, D. Q.; Phillips, J. C.; Lundberg, R. D.; Macknight, W. J.; Chu, B. *Macromolecules* **1989**, *22*, 992.
(32) Moffitt, M.; Yu, Y. S.; Nguyen, D.; Graziano, V.; Schneider, D. K.; Eisenberg, A. *Macromolecules* **1998**, *31*, 2190.
(33) Nguyen, D.; Williams, C. E.; Eisenberg, A. *Macromolecules* **1994**, *27*, 5090.

MA070357O